Comparison of energy distributions of positron- and electron-induced secondary electrons: Implications for slow-positron emission mechanisms

R. Mayer and E. Gramsch
Department of Physics, Brookhaven National Laboratory, Upton, New York 11973

A. Weiss
Department of Physics, University of Texas at Arlington, Arlington, Texas 76019
(Received 15 May 1989)

Positron- and electron-induced secondary-electron-energy distributions have been measured from MgO(100) and Ni(110) crystals. The energy distributions for positron- and electron-induced secondary electrons from MgO and Ni and for the slow-positron emission from the MgO target have been fit by the same analytic function. This analytic function fails to fit the slow-positron energy emission spectrum from Ni. The similarity of positron-induced secondary electron and reemitted positron energy spectra suggests that the slow-positron emission process in ionic insulators may be analogous to secondary-electron generation.

The study of positron-stimulated secondary-electron emission can be expected to illuminate two other important processes to which it bears many analogous features: electron-stimulated secondary-electron emission and low-energy positron reemission from insulators. Positron interactions with matter are in many ways similar to those of the electron except that the positron may be distinguished from the electrons in the material and may have higher collision rates with the target electrons due to their attractive interaction. This makes the positron an interesting probe particle in the study of secondary-electron production. Surprisingly, relatively little work has focused on positron-stimulated secondary-electron production[1-5] and only one study[1,4] has been performed of the energy distribution of secondary electrons resulting from positron bombardment [Cu(100)].

This paper reports the first measurement of positron-induced secondary-electron emission from an insulator surface. In addition, electron-stimulated secondary-electron and slow-positron energy distributions were measured for the same surface in order to facilitate comparisons. The present work finds the shape of the positron- and electron-induced secondary-electron spectra from Ni(110) and MgO(100) and the slow-positron emission spectra from MgO are similar and are not strong functions of incident beam energy. These spectra are vastly different from the energy spectra of positrons reemitted from negative work function metal surfaces [e.g., Ni(110)]. From the shapes of the energy spectra, this paper discusses evidence for a model of positron emission from ionic crystals which is analogous to secondary-electron production. In addition, a first comparison of slow positron and positron-induced secondary-electron yields from van der Waals solids (O_2,N_2) is obtained and a first attempt to characterize an MgO transmission timing remoderator will be reported and discussed.

This study was conducted at the brightness enhanced electrostatically focused beam at Brookhaven National Laboratory.[6] The Ni(110) crystal was heated in a H-Ar mixture for 24 h at 600 °C to eliminate sulfur from the bulk, and was cyclically argon sputtered and annealed at 700 °C in $\sim 2\times 10^{-10}$ torr. The crystal was oriented to within $\leq 2°$. The MgO crystal was 1 mm thick and its back was coated with $\sim$5000-Å copper in order to reduce the problem of charging which was observed in an earlier study.[5] The electron source was extracted from the secondary electrons generated at the last remoderator from the incident 2000-eV positron beam. The integral energy distributions of secondary electrons and reemitted positrons were measured using four-grid low-energy electron diffraction optics mounted on a microchannel plate. As in the previous study,[5] the grids and channel plate were biased in such a way as to permit single-particle detection of electrons or positrons, as appropriate, and to suppress counts due to particles of inappropriate charge.

The integral energy distribution of the emitted particles took a few days to generate due to the low incident beam rates ($\sim$800 counts per second). To directly obtain an energy-distribution spectrum (or derivative of the integral spectrum) with sufficient statistics from the data requires substantially more counts. Often,[7] the derivative spectrum is smoothed to reduce the statistical scatter in the spectrum. Such data manipulation may also introduce extraneous periodic fluctuations depending on the number of channels being averaged in the smoothing scheme. To circumvent this problem, the integral spectrum intensity I (in counts), as a function of emerging particle energy (E), was fitted with an analytic formula of the form

$$I = -0.5N\tanh[(E-E_0)/\sigma]+B,\ E\leq E_0,$$
$$I = -0.5N\{1-\exp[-(E-E_0)/\sigma]\}+B,\ E>E_0, \quad (1)$$

where N is the normalization factor for the integral spectrum, B is the background, E_0 is the energy center for the spectrum, and σ is related to the spread of the spectrum. Equation (1) was fitted to the data using N, B, E_0, and σ as free parameters. This functional form reflects the observed stronger energy dependence in the low-energy portion ($E\leq E_0$) of the spectrum relative to the higher energies ($E>E_0$). The first-order Taylor expansion of Eq.

 ©1989 The American Physical Society

(1) is identical for energies less than and greater than the energy center E_0 and therefore the derivative of the function is continuous at the energy center E_0.

In Fig. 1(a), the experimentally generated integral energy spectra of positron-induced secondary electrons from an MgO crystal is shown along with the fitted spectra (straight line). All spectra shown in this paper were taken using glancing incidence beams ($\theta = 78°$). A small energy offset in the spectra is due to contact potential differences between the sample and the detector grids and does not affect the arguments of this paper because this paper focuses on the general shapes of the energy distributions. The background in the integral spectrum is due to microchannel plate dark counts and long counting times. The instrumental energy resolution is much narrower (< 2 V) than the energy spectra shown in this study and was determined by retracting the sample and measuring the energy spread of the incident beam alone. This energy resolution is somewhat lower than other studies (see Ref. 7) but due to the close comparative nature of this study and the generally broad features of the spectra, it does not affect the conclusions of the paper. To demonstrate the feasibility of the method, the negative derivative spectra is also shown in Fig. 1(a). The derivative spectrum has been rescaled so that the area under the curve is arbitrarily set to one. The derivative spectrum from the fit gives a reasonable description of the experimentally generated derivative. A similar set of curves is shown in Fig. 1(b) for the electron-induced secondary spectrum. The same function [Eq. (1)] is used to fit the data in Fig. 1(b). The energy distribution for a different incident beam energy is shown in Fig. 1(c). It should be noted that there is little difference in the shapes of the energy spectra in Figs. 1(a)–1(e) and they seem to be fitted well by using Eq. (1). Finally, a positron-induced secondary-electron spectrum and a slow-positron emission spectrum generated from Ni and MgO crystals are also shown in Figs. 1(d) and 1(e), respectively, and are fitted with the same function [Eq. (1)]. The data is summarized in Table I by listing the fitted values of the E_0 (the energy center) and the full width at half maximum (FWHM) in the energy-distribution spectrum. The values of E_0 determined from the positron-induced secondary electron spectra are lower than those determined from the electron-induced spectra,

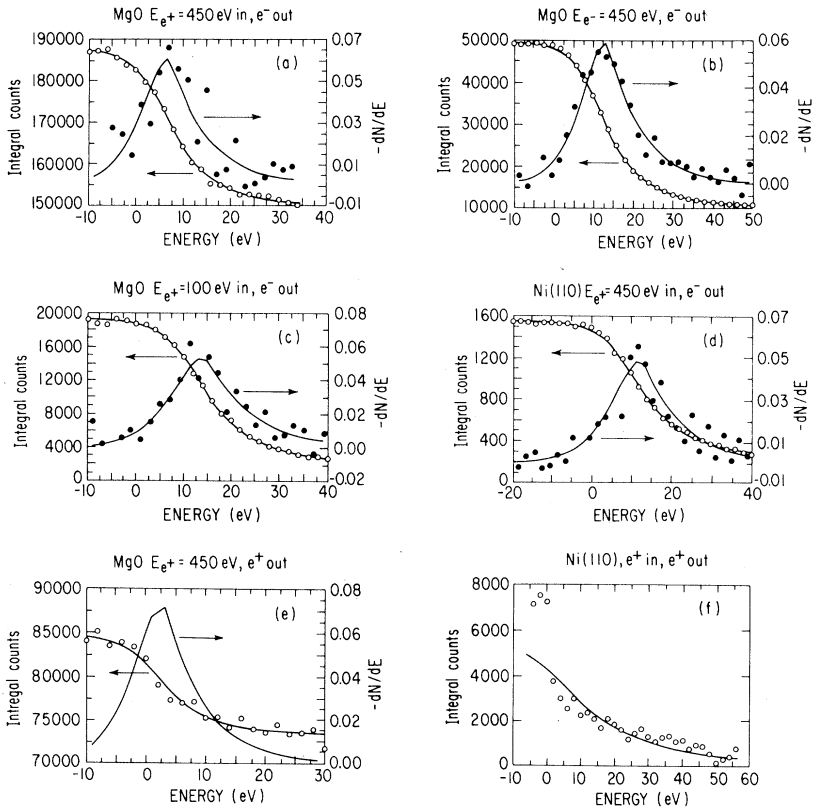

FIG. 1. Integral energy-distribution spectra are denoted by open circles with the left-hand side as its scale, the negative derivatives of the integral spectra are denoted by the filled circles with the right-hand side as its scale and the straight line is a least-squares fit using Eq. (1). All spectra are taken with the same incident beam polar angle and detector position. (a) Positron-induced secondary electrons from MgO crystal for incident beam energy 450 eV. (b) Electron-induced secondary electrons from MgO crystal for incident beam energy 450 eV. (c) Positron-induced secondary electrons from MgO crystal for incident beam energy 100 eV. (d) Positron-induced secondary electrons from a Ni(110) crystal for incident beam energy 450 eV. (e) Slow-positron emission from MgO(100) for positron incident beam energy of 450 eV. (f) Positron emission spectra from Ni(110) crystal for 450-eV incident beam positrons.

TABLE I. Data summary for sample, incident particle type, incident beam energy, emitted particle type, fitted energy center (E_0) for energy distribution of emitted particles, and FWHM for energy distribution of emitted particles.

Sample	Incident particle	Energy (eV)	Emitted particle	Center (eV)	FWHM (eV)
MgO	e^+	100	e^+	7.7	5.35
MgO	e^+	450	e^+	3.0	10.4
MgO	e^+	100	e^-	14.6	14.4
MgO	e^+	450	e^-	7.53	12.7
MgO	e^-	50	e^-	13.1	16.4
MgO	e^-	100	e^-	17.2	20.0
MgO	e^-	450	e^-	13.3	13.2
Ni	e^+	50	e^-	10.3	8.9
Ni	e^+	100	e^-	13.4	12.9
Ni	e^+	450	e^-	12.4	10.1

which are attributed to the absence of back-scattered primary electrons in the positron-induced spectra. The energy distribution of positrons reemitted from negative work function metals surface as exemplified by the spectra from a nickel target [Fig. 1(f)] is very different from those spectra discussed above. As can be seen in Fig. 1(f), the functional form given by Eq. (1) which was successfully used in fitting previous spectra did not provide a good fit to the reemitted positron data from Ni. Earlier studies on Ni(100) (Ref. 8) find a narrow peak at $\sim$0.35 eV with a FWHM of $\sim$0.08 eV in the reemitted energy distribution.

It is interesting to compare our results with previous electron- and proton-induced secondary-electron emission distributions[9] and recall other similar studies. Such reports[10] indicate that the proton- and electron-stimulated secondary-electron energy distributions have similar shapes (which are only weakly dependent on incident beam energy) but with vastly different total yields which is precisely the case in the present study of positron- and electron-induced secondary-electron distributions. Earlier studies[10] found that the high kinetic energy portion of the electron and the proton-induced secondary-electron spectrum could be fitted with an energy dependence of $E^{-1.6}$ or $E^{-1.8}$ behavior. This work finds the high-energy part, $E > E_0$, of the positron- and electron-induced secondary-electron energy distribution decays exponentially [derivative of the high-energy part of Eq. (1)]. This discrepancy (along with variations in peak positrons and widths) may be due to the low incident beam energies (50–450 eV), high incident beam angles (78°), and diminished penetration depths into the sample.

The similarity of the energy spectra of positrons and electrons reemitted from MgO [see Figs. 1(a) and 1(e)] provides evidence that there is a common mechanism leading to the shape of both sets of energy distributions. It is suggested that the shape of the spectra is dominated by the transport properties of nonthermal positrons and electrons, respectively, as they leave the bulk. A similar argument has previously been used to explain the shape of the electron-stimulated secondary-electron spectra using transport theory.[9] In the transport theory[9] for secondary-electron emission, the secondary-electron migration and emission process is separated from the inelastic scattering processes of the incident beam leading to a functional form for the secondary-electron energy spectra that is independent of the incident beam energy. The functional form of the energy distribution, $d\delta/dE_1$ given in Eq. (2), reflects the separation of secondary-electron production into three distinct processes

$$\frac{d\delta}{dE_1} \sim \int_{E_0}^{\infty} d\sigma \left[1 \Big/ \left(\left\| \frac{dE_0}{dx} \right\| \right) \right] (1 - U_0/E_0) , \qquad (2)$$

where (i) the incident beam transfers energy to the electrons in the material, producing secondary electrons whose energy exceeds E_0 (represented by the term $\int_{E_0}^{\infty} d\sigma$), (ii) these electrons may reach the surface and lose energy from $E_0 + dE_0$ to E_0 with a stopping power of $\| dE_0/dx \|$, and finally, (iii) the electrons leave the material with a probability of $(1 - U_0/E_0)$ where U_0 is the electron affinity. It is important to note that processes (ii) and (iii) determine the shape of the energy emission spectrum and are independent of incident beam energy, while (i) only affects the total yield and depends on incident beam energy. This decoupling of the processes is more evident in insulators relative to metals due to the presence of a band gap. Under glancing incidence conditions, Eqs. (1) and (2) imply that for $E_0 \gg U_0$, the secondary-electron energy loss inside the material $\| dE_0/dx \| \sim \exp(E_0/\sigma)$.

The mechanism by which slow positrons are emitted from alkali-metal halide crystals has been the subject of considerable discussion. Originally, Mills and Crane[7] suggested that the anomalously broad and unusual shape of the positron energy emission spectrum from the alkali-metal halide crystals, and incident beam energy-independent energy emission spectrum was due to the ionization of "delocalized" positronium (Ps) (Ref. 11) at the surface and emission of the positron due to the electron from the Ps filling an unfilled electron state at the surface. As in the "hot positron" model of Gullickson and Mills,[12] Lynn and Nielsen[13] suggested that the broad positron energy spectrum in alkali-metal halide crystals was due to the absence of electron-hole pair production mechanisms (and therefore reduction of energy loss and thermalization processes) in insulators for positrons whose energy is less than the band gap of the material and consequently resulting in the emission of nonthermalized positrons. Lynn and Nielsen, however, cited the need for an explanation of the weak dependence of the reemitted positron energy spectra on incident beam energy in ionic solids (the energy distribution of nonthermalized positrons from metals is dependent on the incident beam energy[8]). Such an explanation may be provided by the secondary-electron transport model if the secondary-electron energy distribution is replaced by the energy distribution of positrons after their velocities have been randomized by collisions. The standard treatment for positron emission from metals,[8] unlike the transport theory, assumes short mean free paths for particles returning to the surface relative to the range of the implantation profile and is not valid in materials with long mean free paths such as insulators (due to the absence of electron-hole excitations).

Other studies lend support for the close connection between slow-positron emission and secondary-electron production. The high yields of slow positrons from rare-gas moderators[12,14] and x-ray-induced secondary electrons[15] in xenon have been attributed to the long mean free paths due to the weak phonon interaction with the charged particle. In addition, our comparative measurements[16] from solid O_2,N_2, argon, and neon deposited onto a ^{22}Na positron source found that the total yields of slow positron emission and positron-induced secondaries have roughly the same dependence on sample condition (surface contamination, sample defects, temperature, etc). The molecular van der Waals solids were found to have lower slow positron yields of roughly 14% and 30% for O_2 and N_2, respectively, relative to the argon moderator. It is interesting to note that low electron-induced secondary-electron yields from molecular van der Waals solids were previously[17,18] attributed to the excitation of molecular vibrational levels ($\sim$0.1 eV) which tends to reduce the secondary-electron escape lengths. Such a mechanism is not possible in the rare-gas atom solids, whose escape lengths are determined by the electron-phonon interaction and hence they tend to have long escape lengths and high secondary-electron yields. Similarly, the diffusion lengths for slow positrons in the van der Waals molecular solids should be limited by the excitation of the molecular vibrational spectrum.

Slow-positron moderators used in timing applications generate a "start" signal from secondary electrons induced by moderated positrons.[19] The high-positron stimulated secondary-electron yields from an MgO target therefore suggest that this material may be suitable as an efficient timing transmission moderator. Previously, MgO "smoked" onto a metal had been tested as a back reflection moderator.[20] In preliminary studies, we have thinned a $\sim$1-mm MgO single crystal by depositing it in an 80:20 phosphoric acid-water solution until the crystal is thinned to $\sim$50 μm. Such a thickness is roughly ten times too thick for efficient moderation but mechanically strong enough for transport into a vacuum system. To improve electrical contact and reduce charging problems, $\sim$0.2 μm of copper was evaporated onto the incident beam side of the moderator. Slow-positron yields were measured in a magnetically guided beam[21] following electron-beam heating of the emission side of the moderator to remove surface impurities (such a cleaning procedure may also unfortunately introduce defects into the MgO crystal which can trap positrons). The relative slow/total positron yield is only 2×10^{-5} and has an energy distribution of 4 eV, which is the convolution of the intrinsic energy distribution of the MgO moderator and the instrumental resolution.

In summary, slow-positron emission energy distribution from ionic solids has been compared with the secondary-electron energy distribution and has been found to be very similar in their dependence on the emission energy of the outgoing particle. The shape of the energy spectra from both types of processes were found to be only weakly dependent on the incident beam energy. The energy distribution of slow positrons from Ni(110) is not fitted by the same functional form used to fit the data from ionic solids. These observations suggest that slow-positron emission from ionic crystals, unlike metals, resembles the secondary-electron process as suggested in earlier work on escape lengths in x-ray-stimulated electron production in rare-gas solids.[15]

R.M. and E.G. acknowledge support from the U.S. Department of Energy Contract No. DE-AC02-76-CH00016. A.W. was supported by the Robert A. Welch Foundation, the Texas Advanced Technology Research Program, and the Texas Advanced Research Program.

[1]Alex Weiss, Ph.D. thesis, Brandeis University, 1982 (unpublished).
[2]W. H. Cherry, Ph.D. thesis, Princeton University, 1958 (unpublished).
[3]S. Pendyala, J. Wm. McGowan, P. M. R. Orth, and P. W. Zitzewitz, Rev. Sci. Instrum. **45**, 1347 (1974).
[4]A. Weiss and Karl Canter, in *Proceedings of the Sixth International Conference on Positron Annihilation, Texas, 1982,* edited by P. G. Coleman, S. C. Sharma, and L. M. Diana (North-Holland, Amsterdam, 1982).
[5]Rulon Mayer and Alex Weiss, Phys. Rev. B **38**, 11927 (1988).
[6]W. E. Frieze, D. W. Gidley, and K. G. Lynn, Phys. Rev. B **31**, 5628 (1985).
[7]A. P. Mills and W. S. Crane, Phys. Rev. Lett. **53**, 2165 (1984).
[8]A. P. Mills, Jr., in *Positron Solid State Physics,* edited by W. Brandt and A. Dupasquier (North-Holland, Amsterdam, 1983); P. J. Schultz and K. G. Lynn, Rev. Mod. Phys. **60**, 701 (1988).
[9]Jörgen Schou, Scan. Micros. **2**, 607 (1988).
[10]D. Hasselkamp, S. Hippler, and A. Scharmann, Nucl. Instrum. Methods Phys. Res. Sect. B **18**, 561 (1987).
[11]See, for example, T. Hyodo, in *Proceedings of the Seventh International Conference on Positron Annihilation, ICPA85, New Delhi, 1985,* edited by P. C. Jain, R. M. Singru, and K. P. Gopinathan (World Scientific, Singapore, 1985).
[12]E. M. Gullickson and A. P. Mills, Jr., Phys. Rev. Lett. **57**, 376 (1986).
[13]K. G. Lynn and B. Nielsen, Phys. Rev. Lett. **58**, 81 (1987).
[14]A. P. Mills, Jr. and E. M. Gullickson, Appl. Phys. Lett. **49**, 1121 (1986).
[15]E. M. Gullickson, Phys. Rev. B **37**, 7904 (1988).
[16]R. Mayer and D. Becker (private communication).
[17]H. Sorensen and J. Schou, J. Appl. Phys. **49**, 5311 (1978).
[18]H. Sorensen and J. Schou, J. Appl. Phys. **53**, 5230 (1982).
[19]J. Van House, A. Rich, and P. W. Zitzewitz, Origin Life **14**, 413 (1984).
[20]K. F. Canter, P. G. Coleman, T. C. Griffith, and G. R. Heyland, J. Phys. B **5**, L167 (1972).
[21]E. Gramsch, J. Throwe, and K. G. Lynn, Appl. Phys. Lett. **51**, 1862 (1987).